Environmental Science and Pollution Research (2024) 31:17256–17274
https://doi.org/10.1007/s11356-024-32298-x

RESEARCH ARTICLE

New insights into xenobiotic tolerance of Antarctic bacteria: transcriptomic analysis of *Pseudomonas* sp. TNT3 during 2,4,6-trinitrotoluene biotransformation

Ma. Ángeles Cabrera[1] · Sebastián L. Márquez[1,2] · José M. Pérez-Donoso[1]

Received: 5 July 2023 / Accepted: 28 January 2024 / Published online: 10 February 2024

Abstract
The xenobiotic 2,4,6-trinitrotoluene (TNT) is a highly persistent environmental contaminant, whose biotransformation by microorganisms has attracted renewed attention. In previous research, we reported the discovery of *Pseudomonas* sp. TNT3, the first described Antarctic bacterium with the ability to biotransform TNT. Furthermore, through genomic analysis, we identified distinctive features in this isolate associated with the biotransformation of TNT and other xenobiotics. However, the metabolic pathways and genes active during TNT exposure in this bacterium remained unexplored. In the present transcriptomic study, we used RNA-sequencing to investigate gene expression changes in *Pseudomonas* sp. TNT3 exposed to 100 mg/L of TNT. The results showed differential expression of 194 genes (54 upregulated and 140 downregulated), mostly encoding hypothetical proteins. The most highly upregulated gene (> 1000-fold) encoded an azoreductase enzyme not previously described. Other significantly upregulated genes were associated with (nitro)aromatics detoxification, oxidative, thiol-specific, and nitrosative stress responses, and (nitro)aromatic xenobiotic tolerance via efflux pumps. Most of the downregulated genes were involved in the electron transport chain, pyrroloquinoline quinone (PQQ)-related alcohol oxidation, and motility. These findings highlight a complex cellular response to TNT exposure, with the azoreductase enzyme likely playing a crucial role in TNT biotransformation. Our study provides new insights into the molecular mechanisms of TNT biotransformation and aids in developing effective TNT bioremediation strategies. To the best of our knowledge, this report is the first transcriptomic response analysis of an Antarctic bacterium during TNT biotransformation.

Keywords Transcriptomics · TNT · Xenobiotics · Oxidative stress · Azoreductase · Antarctica · Bioremediation · *Pseudomonas*

Introduction

Since the early twentieth century, the nitroaromatic explosive 2,4,6-trinitrotoluene (TNT) has been extensively used in military and civilian activities (e.g., mining, construction), and its production is still increasing (Maksimova et al. 2018; Lata et al. 2021; Mordor-Intelligence 2021). This has resulted in the release of thousands of tons of TNT and its derivatives into the environment, causing soil and groundwater contamination (Habineza et al. 2017; Chakraborty et al. 2022). Additionally, the adverse effects of TNT on human health and other organisms, such as cytotoxicity and carcinogenicity, have also raised many health concerns (Koske et al. 2019; Thenmozhi and Devasena 2020). Therefore, the removal of TNT from the environment and the restoration of contaminated sites are considered major priorities by the US Agency for Toxic Substances and Disease Registry (ATSDR) (ATSDR 2022).

Since physicochemical methods for TNT removal have proved to be highly cost-intensive and inefficient, bioremediation has emerged as an eco-friendly and sustainable alternative (Claus 2014; Maksimova et al. 2018). The capability of many different bacteria to biotransform or mineralize TNT has been reported, including those of the *Pseudomonas* (Van Dillewijn et al. 2007; Fernández et al. 2009; Cabrera

Responsible Editor: Philippe Garrigues

✉ José M. Pérez-Donoso
jose.perez@unab.cl

[1] Center for Bioinformatics and Integrative Biology (CBIB), Facultad de Ciencias de La Vida, Universidad Andrés Bello, Av. República 330, Santiago, Chile

[2] Fundación Científica y Cultural Biociencia, José Domingo Cañas 2280, Ñuñoa, Santiago, Chile

et al. 2020), *Citrobacter* (Kao et al. 2016), *Bacillus* (Mercimek et al. 2013; Yakovleva et al. 2022), and *Klebsiella* (Kim et al. 2002) genera (Lamba et al. 2022; Gupta et al. 2023b, a; Xu et al. 2023). Nevertheless, the high chemical stability of TNT makes this xenobiotic very difficult to degrade (Lata et al. 2021). In fact, under aerobic conditions, this compound is commonly subjected to reductive attack rather than the usual oxidative degradation that typically occurs with aromatic compounds (Heiss and Knackmuss 2002).

To date, several transcriptomic and proteomic studies providing insights into the bacterial TNT degradation process have been reported, but they remain scarce (Ho et al. 2004; Cho et al. 2009; Fernández et al. 2009; Liao et al. 2018; Xu et al. 2021; Yakovleva et al. 2022). In general, these studies showed the increased expression of genes and proteins related to (nitro)aromatics metabolism (e.g., nitroreductases, Old Yellow Enzymes, azoreductases) and stress response (e.g., thioredoxins, reductases) upon exposure of different bacteria to TNT. Nevertheless, the full set of enzymes and pathways involved in TNT degradation, as well as other related to physiological processes, have not been fully elucidated.

In earlier research, we reported the isolation of the Antarctic bacterium *Pseudomonas* sp. TNT3, which showed remarkable TNT biotransformation capabilities compared to other well-known TNT-degrading bacteria (Cabrera et al. 2020). For further investigation of this phenomenon, in a more recent study, we performed a comparative genomic analysis among TNT-degrading pseudomonads, including *Pseudomonas* sp. TNT3. The results revealed the presence of genes (some of them unique) that are likely to be related to TNT biotransformation (Cabrera et al. 2022). Nonetheless, the changes in gene expression during TNT biotransformation by the isolate TNT3 were not assessed.

The present study aimed to examine the changes in the transcriptome of *Pseudomonas* sp. TNT3 upon exposure to TNT (100 mg/L) in the culture medium under aerobic conditions. Gene expression patterns were analyzed by utilizing RNA sequencing and differential expression analysis. The identification of differentially expressed genes (DEGs) and associated metabolic pathways under the experimental conditions allowed to shed light on the molecular mechanisms utilized by this bacterium to withstand TNT, ultimately contributing to a more comprehensive understanding of the TNT metabolism in bacteria.

Materials and methods

Bacterial growth conditions

The bacterium *Pseudomonas* sp. TNT3 used in this work was previously isolated from Deception Island (Antarctica) in 2018 and then cultured as reported before (Cabrera et al. 2020). Briefly, the bacterial cells were grown in half-diluted R2A medium in the absence and presence of TNT (100 mg/L) at 28 °C using constant agitation. After 8 h of incubation, the culture reached the mid-exponential phase of growth (optical density at 600 nm $= 0.3 \pm 0.01$). This cultivation time was selected since the greatest TNT biotransformation rate by *Pseudomonas* sp. TNT3 was observed here (Cabrera et al. 2020). Three biological replicates per condition were used for further analyses.

TNT quantification

To confirm that TNT was indeed biotransformed by *Pseudomonas* sp. TNT3 during cultivation prior to RNA extraction, the concentration of the remaining TNT in the culture was measured as described before (Cabrera et al. 2020). Briefly, the bacterial cells were centrifuged at 14,000 g× for 10 min. Later, 100 µL of culture supernatant were mixed with 900 µL of 50 mM Tris–HCl buffer (pH 7.0) and then 160 µL of 1 M NaOH were added. The reaction was incubated at 21 °C for 10 min, and the absorbance was measured at 447 nm. Finally, TNT concentration was measured at 0 and 8 h of incubation in the treatment groups.

RNA extraction

Total RNA was performed using the phenol/chloroform method. The bacterial cells were harvested by centrifugation at 14,000 g×, for 10 min, at 4 °C. The cellular pellet was resuspended in lysis buffer (0.5% SDS, 20 mM sodium acetate pH 5.0, 0.3 M sucrose, and 10 mM EDTA in nuclease-free water). The samples were mixed with 500 µL of acid phenol (Sigma Aldrich, USA) and incubated at 65 °C for 5 min. Samples were then vigorously vortexed and incubated on ice for 5 min. Subsequently, the samples were centrifuged at 14,000 g×, for 5 min, at 4 °C, and the aqueous phase was recovered and mixed with 500 µL chloroform. Then, the samples were vortexed vigorously, incubated on ice, and centrifuged under the same conditions. The aqueous phase was recovered, and the RNA was precipitated by adding 2.5 volumes of cold absolute ethanol and then incubated at − 80 °C for 2 h. The samples were centrifuged at 14,000 g×, for 30 min, at 4 °C, and the RNA pellet was dried using a SpeedVac concentrator. Lastly, the RNA was resuspended in 50 µL of nuclease-free water containing 4 U of Ambion™ DNase I (RNase-free) (Ambion, USA).

RNA quantification and integrity

RNA quantification was performed by measuring its absorbance at 260 nm using a Synergy H1 microplate reader (Biotek, USA). The RNA purity was assessed by means of the A260/A280 ratio. Later, the samples with > 1.6 A260/A280 ratio were selected, and their integrity was assessed through capillary gel electrophoresis at the Center of Plant Biotechnology (Universidad Andrés Bello, Santiago, Chile). Lastly, the samples with RNA integrity number (RIN) values > 8 were selected to be sequenced.

RNA sequencing and processing

RNA-seq library preparation and whole transcriptome sequencing by rRNA depletion were performed according to GENEWIZ Company's service (South Plainfield, NJ, USA), for each replicate of treatment and control group. The RNA sequencing of the samples was performed with an Illumina HiSeq 4000 instrument using HiSeq 2×150 PE HO configuration. The quality of raw sequencing data was assessed using FastQC (available at http://www.bioinformatics.babraham.ac.uk/projects/fastqc) and then filtered and trimmed to eliminate low-quality reads and adapters using the BBDuk tool from the BBMap suite (Bushnell 2015) utilizing the following parameters: qtrim-rl to quality-trim both ends, trimq 20 to trim up to quality score of 20, minlen 51 to remove reads of less than 51 bp long after trimming, and k 23 (k-mer size for adapters decontamination). Filtered reads were aligned to the draft genome of *Pseudomonas* sp. TNT3 (GenBank accession: WFGV00000000.2, publicly available) using the short sequence alignment software Bowtie2 (Langmead and Salzberg 2012), and the number of reads mapped to each coding sequence region (coverage) was quantified using the htseq-count tool from HTSeq (Anders et al. 2015) with the intersection-nonempty mode to deal with multi-mapping reads. Samtools (Danecek et al. 2021) was used for manipulation of mapping files. The resulting read count matrix was used for downstream differential gene expression analysis with DeSeq2 package according to Love et al. (2014). Changes in gene expression levels were expressed as the $\log_2$-fold change ($\log_2$FC) resulting from applying a Benjamini-Hochberg (BH) false discovery rate (FDR) correction of Wald test *p*-values for multiple testing at 5%. A gene was considered as differentially expressed gene (DEG) when its adjusted *p*-value was below 0.05 (adjusted *p*-value ≤ 0.05) and the expression level exceeded a 2.8-fold change ($|\log_2 FC| \geq 1.5$) between control and treatment groups.

Functional annotation

The functions of the DEGs were annotated using public databases including the Kyoto Encyclopedia of Genes and Genomes (KEGG) (Kanehisa et al. 2023), Clusters of Orthologous Groups (COG) (Galperin et al. 2021), and Gene Ontology (GO) (Carbon et al. 2021) through the FACoP web server (De Jong et al. 2022). UniProt Knowledgebase database (UniProtKB) (Bateman et al. 2023) and InterPro databases (Paysan-Lafosse et al. 2023) were also used to analyze amino acid sequences. For each COG, KEGG, and GO term, the gene count was compared between the treatment and control conditions. GO terms over-representation analysis and KEGG pathway enrichment analysis were performed using Bioconductor's clusterprofileR (Yu et al. 2012).

Results and discussion

RNA-seq analysis of the *Pseudomonas* sp. TNT3 transcriptome in the presence of TNT

To investigate the metabolic response of *Pseudomonas* sp. TNT3 to TNT exposure, RNA-seq transcriptome analysis was performed on samples from cultures induced with an initial TNT concentration of 100 mg/L. Control (without TNT) and treatment (induced with TNT) samples for total RNA extraction were collected after 8 h of culture, when the cultures had reached the mid-exponential phase. Quantification of TNT in the cultures showed that after 8 h, *Pseudomonas* sp. TNT3 biotransformed approximately 20% of the compound.

Later, six cDNA libraries were generated and sequenced (three from the TNT-induced samples and three from the control samples), resulting in an average of 22 million raw reads per sample. After quality control and trimming, approximately 1 million reads were filtered out from each sample, and the average quality score and length of the remaining reads were > Q30 and 130 bp, respectively. Cleaned reads were successfully mapped to the 6120 coding sequences (CDSs) previously predicted for the reference genome (Cabrera et al. 2022) with Bowtie2, resulting in 6114 genes with a nonzero count and an average overall alignment rate of 99% (Table S1). A matrix of read counts per gene was generated for each sample using HTSeq and then transformed into a DESeq2 object for gene expression value estimation. The similarity of the sample replicates from each group was assessed by means of hierarchical clustering and principal component analysis (PCA) of the regularized log-transformed data to check how similar the replicates were to each other and to ensure that the treatment condition was the major source of variation, respectively. As a result, both clustering and PCA showed that the treated and control samples were clearly clustered into two separate groups by condition (control and TNT treatment), indicating a high degree of similarity between the replicates of the raw data (Fig. S1).

Differential expression analysis

Differential expression analysis was performed based on the negative binomial distribution, as implemented in DESeq2. Genes showing > 2.8-fold change ($|\log_2FC| \geq 1.5$) between control and treatment conditions at FDR-corrected *p*-value < 0.05 were considered as DEGs. As a result, 194 genes out of 6114 with non-zero counts were differentially expressed upon exposure to TNT, corresponding to 3% of the total genes predicted for *Pseudomonas* sp. TNT3 (a complete list of up- and downregulated genes and their respective annotations is attached as Supplementary Material). The analysis also showed that the downregulated genes comprised a higher fraction (72%, or 140 genes) than upregulated genes (28%, or 54 genes). The volcano plot in Fig. 1 illustrates the expression distribution of DEGs. Additionally, a heatmap showing the normalized expression of the top 50 most significant genes was generated (Fig. S2). The small proportion of DEGs upon exposure to TNT with respect to the total predicted CDSs (only 3.2% of 6114 genes with nonzero transcript counts) suggests that this isolate may have a limited set of genes that are specifically involved in responding to this xenobiotic. In addition, the observed change in expression was notably higher for the downregulated genes than for upregulated genes. As suggested by Xu et al. (2021), the first steps of TNT metabolism may be carried out by a limited number of enzymes whose products are further degraded by central metabolic routes such as the β-ketoadipate pathway.

Functional classification of DEGs into Clusters of Orthologous Groups (COGs)

DEGs were categorized into COG functional categories according to eggNOG annotation. As a result, they were classified into 19 categories, with the most enriched being [S] "unknown function" (20%), followed by [E] "amino acid metabolism and transport" (10%), and [M] "cell wall/membrane/envelope biogenesis" (10%). As shown in Fig. 2a, downregulated genes in these three categories were much more abundant than those upregulated. This difference suggests that the downregulation of certain genes involved in central metabolism may be key to reducing energetic costs and allocating energy to the degradation of TNT and the concomitant stress-related response. Interestingly, several DEGs with high levels of expression (> 2.8-fold change) classified into the [S] category were, in fact, genes with known functions according to their Rapid Annotation using Subsystem Technology (RAST) annotations, such as those encoding proteins involved in the degradation pathway of the aromatic compound phenylacetate (e.g., 1,2-phenylacetyl-CoA epoxidase), as discussed below (Table 1).

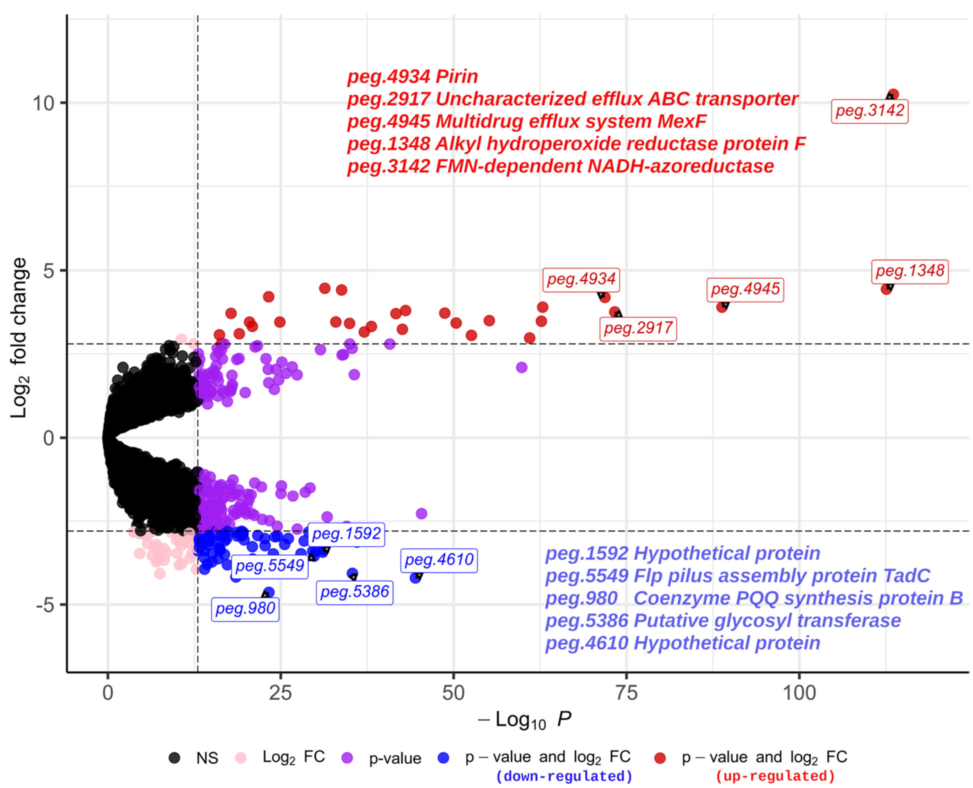

Fig. 1 Differential expression analysis of *Pseudomonas* sp. TNT3 genes in response to TNT exposure. The volcano plot shows the DEGs of *Pseudomonas* sp. TNT3 cells in response to the TNT exposure (100 mg/L) compared to control conditions (untreated). The *y*-axis ($\log_2$-fold change) represents the difference in the expression level of each gene between the two conditions. The red and blue dots represent the upregulated and downregulated DEGs based on a 2.8-fold difference in expression, respectively (dashed horizontal lines); the *x*-axis (−log10 *p*-value) represents the level of significance of each gene. The dashed vertical line represents a cutoff of 10e − 14. The top five most upregulated and downregulated genes (based on an FDR cutoff of 0.05) are labeled in red and blue, respectively

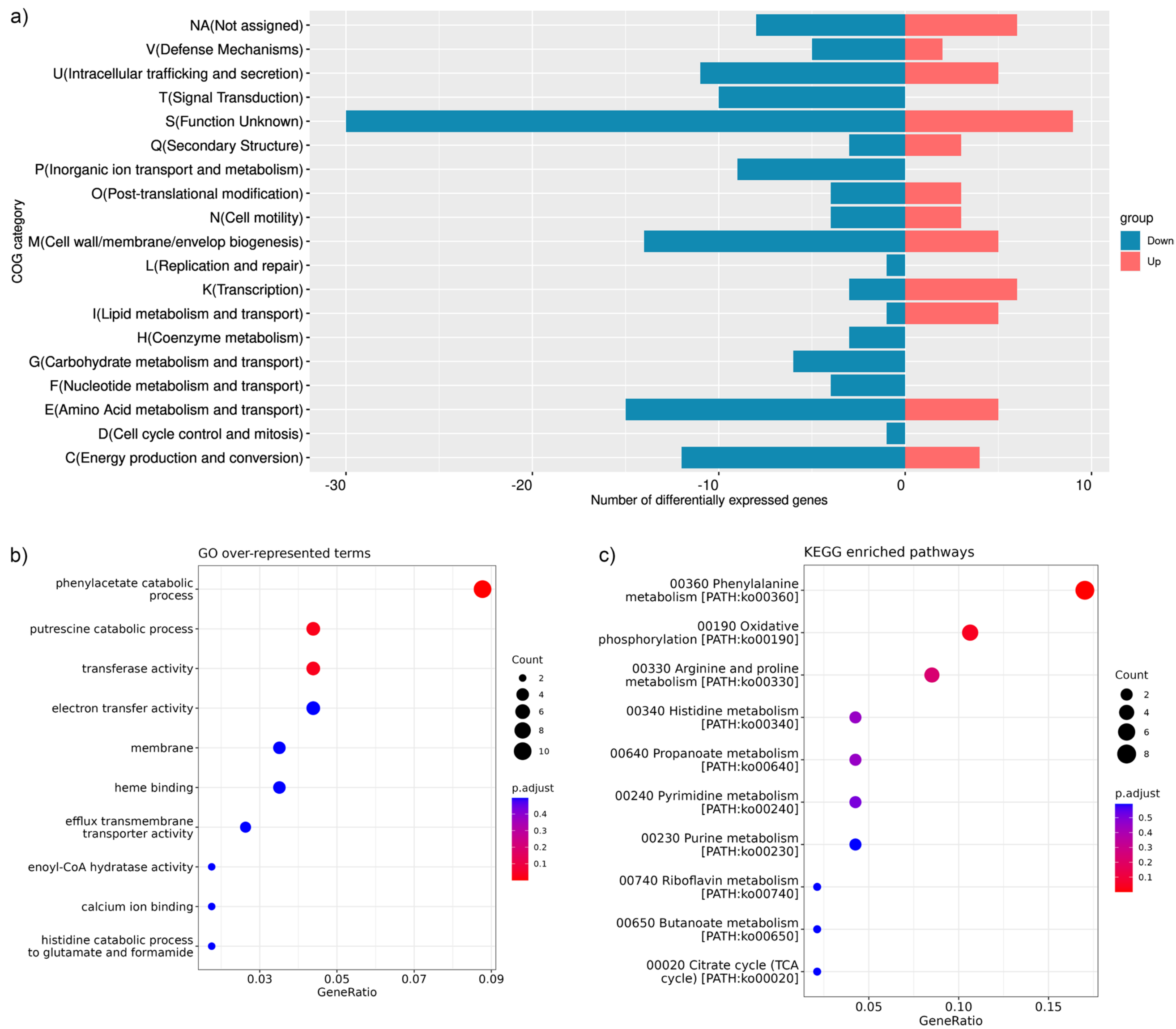

Fig. 2 Functional annotation and over-representation/enrichment analysis of the DEGs. **a** Bidirectional bar chart showing the classification of the DEGs into Clusters of Orthologous Groups (COG) according to egg-NOG annotation. **b** Gene ontology (GO) over-representation analysis. Only the top 10 over-represented GO-terms are shown. Gene ratio is the percentage of total DEGs in the given GO term. **c** Kyoto Encyclopedia of Genes and Genomes (KEGG) enrichment analysis. Only the top 10 most enriched pathways are shown. The color gradient represents the false discovery rate (*p*-adjusted), from the lowest (red) to the highest (blue), respectively. The number of genes in each term/category is represented by the sizes of the circles

Gene ontology (GO) terms enrichment analysis

After annotation of DEGs with the FACoP server, a GO term over-representation analysis was performed using the Bioconductor's clusterProfiler package (Fig. 2b). As a result, we found that among the ten most enriched GO terms, the most significant were those belonging to the biological processes "phenylacetate catabolic process" (24%), and "putrescine catabolic process" (12%). Although it has been described that phenylacetate is one of the compounds into which TNT can be converted under anaerobic conditions (Shen et al. 2000), some facultative anaerobes (e.g., several *Pseudomonas* species) possess genes for both aerobic and anaerobic toluene degradation and are capable of biotransforming this compound by carboxylation to phenylacetate via the phenylacetate pathway (Ganesh Kumar et al. 2019). The latter route combines both aerobic and anaerobic properties for the degradation of aromatic compounds (Nogales et al. 2017).

Regarding the GO term "putrescine catabolic process," it has been described that the catabolism of putrescine is a core metabolic response to oxidative stress (Schneider

Table 1 List of the most upregulated DEGs in *Pseudomonas* sp. TNT3 grown in the presence of TNT. No annotation (N.A.)

Process	Gene ID	RAST annotation	PROKKA annotation	Protein function	log_2FC
Detoxification	peg.3142	FMN-dependent NADH-azoreductase (EC 1.7.1.6)	FMN-dependent NADH-azoreductase 1	Azo compounds and TNT degradation (Liu et al. 2007; Mercier et al. 2013; Misal and Gawai 2018)	10.4
	peg.1349	Alkyl hydroperoxide reductase protein C (AhpC) (EC 1.11.1.15)	Alkyl hydroperoxide reductase C	Peroxidase involved in cell protection against oxidative stress by detoxifying H_2O_2 (Seaver and Imlay 2001)	4.6
	peg.1348	Alkyl hydroperoxide reductase protein F (AhpF)	Alkyl hydroperoxide reductase subunit F	Cell protection against DNA damage in conjunction with AhpC (Rocha and Smith 1999; Seaver and Imlay 2001)	4.4
	peg.4934	Pirin	Quercetin 2,3-dioxygenase	Oxidative stress response (Talà et al. 2018). Oxidation of methyl group in TNT derivatives?	4.3
	peg.4907	1,2-Phenylacetyl-CoA epoxidase, subunit A (EC 1.14.13.149)	1,2-Phenylacetyl-CoA epoxidase, subunit A	Phenylacetate degradation. PaaABCE monooxygenase (Teufel et al. 2010; Grishin and Cygler 2015)	3.8
	peg.4908	1,2-Phenylacetyl-CoA epoxidase, subunit B (EC 1.14.13.149)	1,2-Phenylacetyl-CoA epoxidase, subunit B	Phenylacetate degradation. PaaABCE monooxygenase (Teufel et al. 2010; Grishin and Cygler 2015)	3.8
	peg.3680	Oxidoreductase	Gamma-glutamylputrescine oxidoreductase	Nitrogen metabolism and/or oxidative stress response?	3.5
	peg.4909	1,2-Phenylacetyl-CoA epoxidase, subunit C (EC 1.14.13.149)	1,2-Phenylacetyl-CoA epoxidase, subunit C	Phenylacetate degradation. PaaABCE monooxygenase (Teufel et al. 2010; Grishin and Cygler 2015)	3.4
	peg.5858	1,2-Epoxyphenylacetyl-CoA isomerase (EC 5.3.3.18)	N.A	Phenylacetate degradation (Teufel et al. 2010)	3.4
	peg.6105	3-Hydroxyadipyl-CoA dehydrogenase	N.A	Phenylacetate degradation (Teufel et al. 2010)	3.2
	peg.4910	1,2-Phenylacetyl-CoA epoxidase, subunit D (EC 1.14.13.149)	Putative 1,2-phenylacetyl-CoA epoxidase, subunit D	Phenylacetate degradation (Teufel et al. 2010)	3.0

Table 1 (continued)

Process	Gene ID	RAST annotation	PROKKA annotation	Protein function	log_2FC
Membrane transport	peg.4945	Multidrug efflux system, inner membrane proton/drug antiporter (RND type) ≥ MexF of MexEF-OprN system	Efflux pump membrane transporter BepE	Multidrug resistance (antibiotics with nitro groups), cell protection against nitrosative stress (Juarez 2017)	3.9
	peg.4946	Multidrug efflux system, membrane fusion component = > MexE of MexEF-OprN system	Efflux pump periplasmic linker BepF	Multidrug resistance (antibiotics with nitro groups), cell protection against nitrosative stress (Juarez 2017)	3.5
	peg.4944	Multidrug efflux system, outer membrane factor lipoprotein = > OprN of MexEF-OprN system	N.A	Multidrug resistance (antibiotics with nitro groups), cell protection against nitrosative stress (Juarez 2017)	3.0
	peg.2917	Uncharacterized efflux ABC transporter, ATP-binding protein YadG	Putative ABC transporter ATP-binding protein YadG	Subunit of the YadGH drug transporter (Moussatova et al. 2008). The promoter of the *yadG* gene senses TNT and DNTs (Tan et al. 2015)	3.8
	peg.2918	Uncharacterized efflux ABC transporter, permease protein YadH	Inner membrane transport permease YadH	Subunit of the YadGH drug transporter (Moussatova et al. 2008)	2.8
	peg.3048	Multidrug efflux system EmrAB-OMF, membrane fusion component EmrA	Putative multidrug resistance protein EmrK	Resistance against various dyes, ionophores, and detergents (Zgurskaya 2009)	3.5
	peg.5682	Outer membrane factor (OMF) lipoprotein associated with EmrAB-OMF efflux system	N.A	Resistance against various dyes, ionophores, and detergents (Zgurskaya 2009)	2.5
Unknown	peg.1879	Hypothetical protein	Hypothetical protein	Part of a transmembrane transporter involved in the extrusion of TNT and/or its metabolites?	4.7
	peg.1079	Hypothetical protein	Hypothetical protein	Small membrane protein that regulates the degradation of aromatic compounds?	4.5
	peg.1080	Hypothetical protein	Hypothetical protein	Small membrane protein that regulates the degradation of aromatic compounds?	3.6
	peg.1078	Hypothetical protein	Hypothetical protein	Small membrane protein that regulates the degradation of aromatic compounds?	3.5

et al. 2013), such as that resulting from the degradation of aromatic compounds like TNT (Fernández et al. 2009; Liao et al. 2018; Xu et al. 2021). Putrescine is the metabolic precursor of spermidine and spermine, polyamines that, due to their higher number of positive charges, favor the maintenance of cellular reactive oxygen species (ROS) homeostasis by binding to polyanionic biomolecules like DNA, RNA, proteins, and lipids (Solmi et al. 2023). A recent study by Solmi et al. (2023) in *Pseudomonas syringae* demonstrated that this bacterium responds to oxidative stress by increasing the extracellular levels of putrescine, while maintaining the intracellular levels of spermidine.

Additionally, the GO molecular function "transferase activity" was also enriched (12%). Over-representation of this latter term was expected because several of these enzymes (e.g., acetyl transferases and glutathione transferases) play crucial roles in the detoxification of aromatic compounds (Allocati et al. 2009; Durante-Rodríguez et al. 2017).

KEGG enrichment analysis

The over-regulated DEGs were also classified into KEGG pathways using the FACoP server for enrichment analysis using the *enricher* function from Bioconductor's clusterProfiler package (Fig. 2c). As a result, we observed that most of the DEGs in the top 10 most enriched pathways were involved in those related to "phenylalanine metabolism" (30%), "oxidative phosphorylation" (18%), and "arginine and proline metabolism" (15%). These results are consistent with those of GO enrichment analysis, since the "phenylalanine metabolism" KEGG pathway includes the "phenylacetate degradation" module (M00878), a route used by several bacteria to degrade aromatic compounds (Nogales et al. 2017). Regarding the "oxidative phosphorylation," it has been described that the exposure to xenobiotics can lead to the over-regulation of genes belonging to this key pathway in bacteria, such as those encoding cytochrome *c* oxidases (Fernández et al. 2009; Liu et al. 2017). Lastly, the enrichment of the "arginine and proline metabolism" pathway, which involves the "polyamine biosynthesis" modules (M00133 and M00134), is consistent with the results of GO enrichment analysis since polyamines (e.g., putrescine) catabolism participate in the protection of bacterial cells against oxidative stress (Solmi et al. 2023).

Upregulated DEGs in response to TNT exposure

Using the functional annotation of DEGs, we further analyzed the specific functions that they may be performing in the metabolic processes and pathways. As a result, we found that most of the upregulated DEGs encoded enzymes related to xenobiotic detoxification (e.g., nitroaromatic compounds and phenylacetate), cell protection against oxidative stress (such as that caused by TNT metabolism), and membrane transport processes (efflux pumps that extrude xenobiotics) (Fig. 3; Fig. 4; Table 1). The differential gene expression pattern was broadly similar to that reported in other transcriptomic studies of bacteria exposed to TNT (Fernández et al. 2009; Liao et al. 2018; Xu et al. 2021). The functions of the DEGs with the highest fold changes are described below.

DEGs encoding detoxification enzymes

The differential expression analysis showed a significant upregulation (> 1300-fold change) of a gene (gene ID: peg.3142) that encodes an FMN-dependent NADH azoreductase (AzoR) (Fig. 1; Table 1; Table 2), named "AzoR-a" in our previous work (Cabrera et al. 2022). AzoRs are enzymes that can reduce the azo bond ($R-N=N-R'$) of aromatic azo dyes, converting them into the corresponding amines. During TNT biotransformation, the spontaneous condensation of partially reduced TNT derivatives, such as HADNTs and nitroso-toluenes produces azoxy compounds, which then are biotransformed into azo compounds. These metabolites are even more toxic than TNT to the cell (Haïdour and Ramos 1996; Hawari et al. 2000; Lata et al. 2021). Hence, AzoR could be playing a role in the detoxification of these metabolites.

It has also been reported that AzoRs possess nitroreductase activity, which involves the reduction of nitro groups of some nitroaromatic compounds (Mercier et al. 2013; Misal and Gawai 2018). Although the nitroreductase activity of AzoRs toward TNT has not been extensively studied, it has been shown to play a role in the metabolism of this xenobiotic. This is supported by the upregulation of an azoR gene or the overexpression of the enzyme in transcriptomic and proteomic analyses when bacteria have been exposed to TNT (Fernández et al. 2009; Yakovleva et al. 2022), which is in agreement with our results. Furthermore, AzoR from *Rhodobacter sphaeroides* AS1.1737 has been shown to perform the nitroreduction of TNT (a pathway carried out by nitroreductases), converting it to hydroxylaminodinitrotoluenes (HADNTs) (Liu et al. 2007). In addition, an *Escherichia coli* biosensor strain with a plasmid containing an *azoR* promoter that responds to TNT and 2,4-dinitrotoluene has been reported (Henshke et al. 2021).

Remarkably, the AzoR enzyme identified in the isolate TNT3 exhibits a noteworthy 37% sequence similarity with the AzoR enzyme found in *R. sphaeroides* AS1.1737. Moreover, several crucial residues involved in cofactor (FMN) binding and several conserved residues are present as previously reported (Liu et al. 2007; Gonçalves et al. 2013) (Fig. S3). Furthermore, upon analyzing the genomic context of peg.3142, it was found to be next to a gene encoding a dienelactone hydrolase (Fig. S4) involved in the

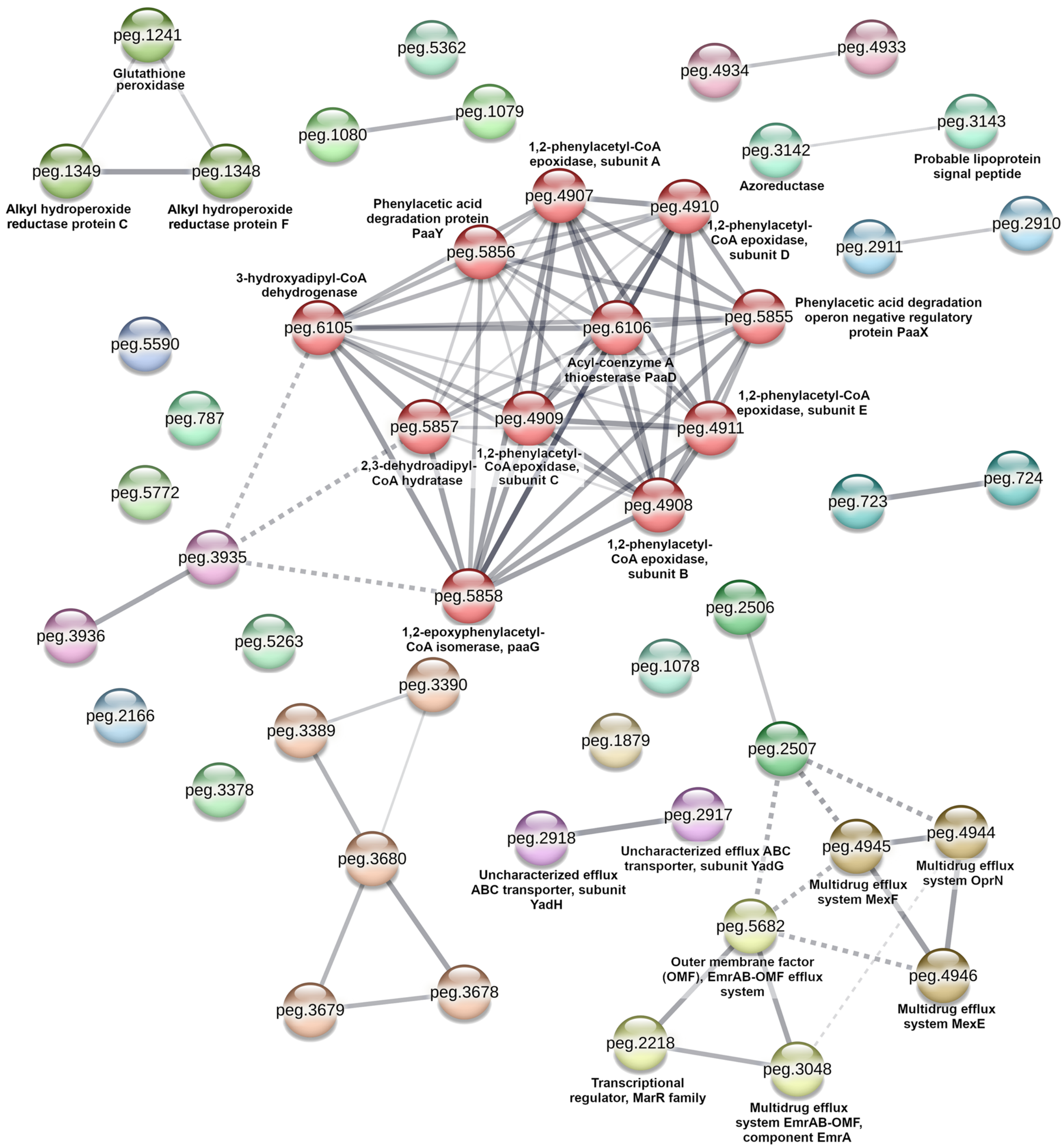

Fig. 3 STRING protein–protein interaction network of upregulated DEGs. Each network node represents a protein encoded by an upregulated differentially expressed gene (p-adjusted < 0.05, $|\log_2(FC)| > 1.5$). The thickness of the gray lines represents the confidence of the data supporting a protein–protein interaction, inferred considering both functional and physical protein associations (full STRING). The network was clustered to a Markov clustering (MCL) inflation parameter of 3, resulting in 13 clusters; each one represented in a different color. Dashed lines represent edges between clusters

biodegradation of chloroaromatic pollutants (Nogales et al. 2017). As we reported before, TNT3 also demonstrates the ability to catalyze the nitroreduction of TNT, resulting in the production of 2-amino-4,6-dinitrotoluene (2-ADNT), a metabolite derived from the reduction of 2-HADNT (Cabrera et al. 2020). This capability could be attributed, at least in part, to the nitroreductase activity exhibited by the AzoR enzyme encoded by the gene peg.3142. It is important

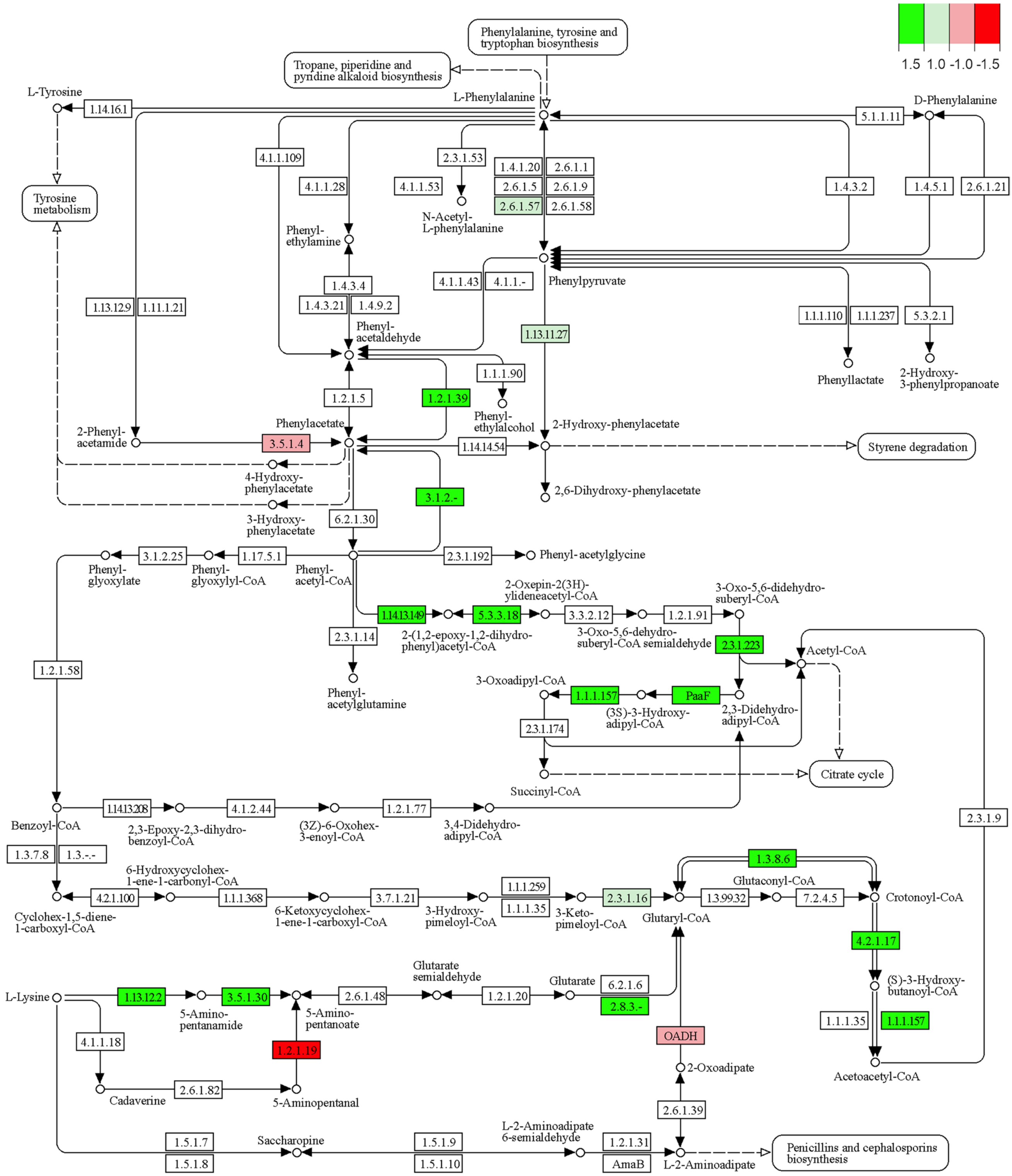

Fig. 4 KEGG pathview graph of representative metabolic routes where DEGs are present. Red denotes downregulation, and green denotes upregulation of genes/transcripts ($|\log_2(FC)| > 1.5$). Light colors represent lower expression values ($|\log_2(FC)| > 1.0$). KO terms were assigned to the protein sequences encoded by the DEGs and subsequently mapped to their respective pathways using BlastKOALA

Table 2 List of oxidoreductases and oxygenases potentially involved in TNT metabolism when *Pseudomonas* sp. TNT3 is grown in the presence of the xenobiotic

Gene ID	Annotation (RAST)	UniProtKB	Motif search (KEGG)	InterPro	Fasta search (KEGG)	KEGG KO
peg.3142	FMN-dependent NADH-azoreductase (EC 1.7.1.6)	88% identity with an FMN-dependent NADH:quinone oxidoreductase 3 (Q3KD08) from *Pseudomonas fluorescens* (strain Pf0-1),	NADPH-dependent FMN reductase (Pfam: PF03358)	Family: NADH:quinone oxidoreductase, FMN-dependent (IPR023048). Domain: Flavodoxin-like fold (IPR003680)	FMN-dependent NADH-azoreductase (NK667_11920) from *Pseudomonas nunensis*	K01118 (FMN-dependent NADH-azoreductase [EC:1.7.1.17])
peg.4934	Pirin	89% identity with a Quercetin 2,3-dioxygenase (A0A0C5ECP9) from *Pseudomonas* sp. MRSN 12121. Pirin N- and C-terminal domain	Pirin-related protein (NCBI-CDD: 224655). Pirin (Pfam: PF02678)	Family: Pirin (IPR012093). Domain: Pirin C-terminal (IPR008778)	Quercetin 2,3-dioxygenase (PFAS1_02575) from *Pseudomonas frederiksbergensis*	K06911 (quercetin 2,3-dioxygenase [EC:1.13.11.24])
peg.3680	Oxidoreductase	87% identity with a FAD-dependent oxidoreductase (A0A010SSI1) from *P. fluorescens* HK44. FAD-dependent oxidoreductase domain	FAD dependent oxidoreductase (Pfam: PF01266)	Domain: FAD dependent oxidoreductase (IPR006076). Sarcosine dehydrogenase-related (PTHR13847)	FAD-dependent oxidoreductase (PFAS1_22905) from *P. frederiksbergensis*	No assigned

to mention that although TNT3 possesses genes encoding enzymes potentially involved in the direct biotransformation of TNT, such as nitroreductases, Old Yellow Enzymes, and azoRs (Cabrera et al. 2022), only peg.3142 was found to be upregulated in the experimental conditions tested. However, it is likely that the other enzymes may be acting at earlier or later steps of TNT biotransformation.

Another upregulated DEG (gene ID: peg.1349) was that encoding an alkyl hydroperoxide reductase (Ahp). This enzyme is a NAD(P)H-dependent peroxidase that catalyzes the reduction of hydrogen peroxide (H_2O_2) and organic hydroperoxides such as lipid peroxides (Rocha and Smith 1999; Seaver and Imlay 2001). It consists of AhpC and AhpF subunits that work together to protect the cell from ROS and reactive nitrogen species (RNS), such as nitric oxide ($NO^{\cdot}$) and nitrogen dioxide ($NO_2^{\cdot}$). Both ROS and RNS are known to cause damage to DNA, proteins, and cell membranes (Chen et al. 1998; Rocha and Smith 1999; Poole 2012; Juarez 2017). Previous studies have shown that the degradation of TNT leads to oxidative and nitrosative stress due to the oxidation of the aromatic ring and the reduction of nitro groups, respectively (Esteve-Núñez et al. 2001; Kumagai and Shimojo 2002; Ladino-Orjuela et al. 2016). Thus, our findings are consistent with previous reports in bacteria exposed to aromatic xenobiotics, including TNT (Cho et al. 2009; Liu et al. 2017; Ortiz-Hernández et al. 2021). Therefore, the Ahp enzyme in the isolate TNT3 may function as a defensive mechanism that protects biomolecules from ROS and RNS produced during TNT biotransformation.

We also observed that a considerable number of upregulated DEGs encode enzymes related to the phenylacetate degradation route (Fig. 3; Fig. 4; Table 1). This pathway is the core of the phenylacetyl-CoA catabolon, a functional unit that comprises several catabolic pathways that transform structurally related aromatic compounds (e.g., styrene, ethylbenzene, phenylacetyl esters) into the common intermediate phenylacetyl-CoA. The latter is then converted into other metabolites that enter the tricarboxylic acid (TCA) cycle (Luengo et al. 2001). Although the degradation of TNT by this catabolon has not yet been established, given the structural resemblance between TNT and ethylbenzene, it is plausible that certain TNT metabolites lacking nitro groups may enter the phenylacetate pathway.

In the process of converting these TNT metabolites to phenylacetate-like derivatives, their methyl group should be oxidized to methyl alcohol. We propose that this process may be facilitated by the upregulated DEG peg.4934 ($log_2FC = 4.2$) encoding a pirin enzyme in *Pseudomonas* sp. TNT3 (Table 1). Pirins are multifunction proteins involved in the oxidative stress response (Talà et al. 2018), but they also exhibit quercetin 2,3-dioxygenase activity, contributing to the reduction of polyphenolic compounds

(Adams and Jia 2005; Widiatningrum et al. 2015; Wang 2022). In the case of peg.4934, its gene product shares 89% identity with a Quercetin 2,3-dioxygenase (UniProtKB: A0A0C5ECP9) of *Pseudomonas* sp. MRSN 12121 (Table 2). Additionally, when analyzing the genomic context of this DEG, we observe its proximity to a gene encoding a γ-Carboxymuconolactone, an enzyme implicated in the benzoate degradation pathway (Nogales et al. 2017). Additionally, it is situated in close proximity to three upregulated DEGs encoding the multidrug efflux pump MexEF-OprN, responsible for expelling nitroaromatic compounds (Fetar et al. 2011; Juarez 2017).

It is noteworthy that certain dioxygenases involved in TNT biotransformation in certain TNT-degrading bacteria also possess the capability to oxidize the methyl group of 2-amino-4,6-dinitrotoluene (2-ADNT) to form a methyl alcohol group as a secondary reaction (Johnson et al. 2001; Keenan and Wood 2006). Given our previous identification of 2-ADNT as a TNT derivative in our isolate (Cabrera et al. 2020), the upregulation of peg.4934 suggests a plausible mechanism for the oxidation of methyl groups in TNT metabolites.

Presuming that TNT derivatives are subject to biotransformation in a manner analogous to ethylbenzene, a compound structurally similar to denitrated TNT derivatives, the benzyl alcohol compound should then be oxidized to aldehyde and subsequently be further oxidized to carboxylic acid, ultimately entering the phenylacetate pathway (Luengo et al. 2001). Although the analysis of upregulated DEGs did not yield an alcohol dehydrogenase, we did identify a phenylacetaldehyde dehydrogenase encoded by peg.5362 ($\log_2 FC = 2.7$) that could be performing the latter step.

Considering the origin of our isolate, the possibility persists that it may harbor novel enzymes or uncharacterized metabolic pathways responsible for the oxidation of methyl groups in TNT derivatives. Nonetheless, a more in-depth investigation is imperative to elucidate these potential enzymatic processes.

Another notably upregulated DEG was peg.3680, which encodes an oxidoreductase (Table 1; Table 2; Fig. S5). The enzyme sequence was analyzed using the InterPro server, revealing the presence of a FAD-binding conserved domain. Through a genomic context analysis of peg.3680, we identified adjacent genes encoding a "glutamine synthetase family protein" under the regulation of a "transcriptional regulator, MerR family." Since glutamine synthetases are involved in nitrogen metabolism and oxidative stress response, the close proximity of peg.3680 to these genes implies its potential involvement in the assimilation of nitrogen (from the nitrite released during TNT biotransformation) via the GS-GOGAT pathway as proposed before (Brown et al. 2003; Habineza et al. 2017; Aldarini et al. 2017; Cabrera et al. 2020).

DEGs related to membrane transport

Another group of DEGs that responded to TNT exposure encoded for membrane transporters, including efflux pumps. Among these transporters, MexEF-OprN, YadGH, and EmrAB-OMF, which have been previously characterized in various organisms, are particularly noteworthy (Fig. 3; Table 1). The MexEF-OprN efflux pump, belonging to the resistance-nodulation-cell division (RND) family, is a tripartite system composed of MexE, MexF, and OprN components (encoded in an operon). This efflux pump can extrude a variety of antibiotics, such as the nitroaromatic compound chloramphenicol (Juarez 2017). Studies by Fetar et al. (2011) and Juarez (2017) have reported that the expression of this pump is induced by nitrosative and thiol stress caused by nitroaromatic compounds and quinones, respectively. Hence, the upregulation of the MexEF-oprN operon in response to TNT exposure may be attributed to the generation of reactive nitrogen species and quinones during TNT biotransformation. This finding is consistent with a previous study conducted on *P. putida* KT2440 exposed to TNT (Fernández et al. 2009).

Additionally, two genes encoding a YadGH efflux transporter were also upregulated. YadGH is a member of the ATP-binding cassette (ABC) transporters superfamily, comprising two subunits, YadG and YadH, that translocate diverse substrates across the cell membrane, such as xenobiotics (Thomas and Tampé 2020). The promoter of the *yadG* gene has been shown to exhibit high sensitivity to TNT and its metabolite 2,4-dinitrotoluene in *E. coli* K-12 MG1655, which was constructed as a TNT biosensor (Tan et al. 2015). While the upregulation of the *yadGH* genes has not been previously reported in transcriptomic studies using TNT, increased levels of ABC transporter transcripts or proteins have been observed in bacteria exposed to TNT (Liao et al. 2018; Yakovleva et al. 2022).

The third upregulated transporter was an EmrAB-OMF multidrug efflux pump, belonging to the major facilitator superfamily (MFS), that is known to extrude various dyes, ionophores, and detergents (Zgurskaya 2009). Although EmrAB-OMF has not been linked to TNT degradation, its genic expression can be induced by 2,4-dinitrophenol, a nitroaromatic compound that possesses a very similar structure to 2,4-dinitrotoluene (2,4-DNT), a TNT metabolite (Xiong et al. 2000; Esteve-Núñez et al. 2001). Hence, it is plausible that the upregulation of the gene encoding the EmrAB-OMF transporter in the isolate TNT3 is induced by 2,4-DNT.

Highly upregulated DEGs encoding hypothetical proteins

A third group of DEGs that exhibited significant upregulation in this study are those that encode hypothetical proteins, as shown in Table 1. Notably, several of these proteins are potentially associated with the cell membrane, and their $\log_2$ fold-change values are comparable to those involved in cell detoxification and membrane transport, according to GO annotations. Consequently, these proteins were subjected to further scrutiny.

Examination of the gene context surrounding the most highly upregulated gene (peg.1879, $\log_2FC = 4.7$) that encodes a hypothetical protein (hp_1879), as presented in Table 1, revealed its proximity to genes linked to xenobiotic metabolism. For example, the gene encoding the transcriptional regulator AcrR is located adjacent to this gene, as depicted in Fig. S6. This type of transcriptional factors is mainly involved in multidrug resistance (Perez-Rueda et al. 2018) and, particularly, it has been described that AcrR represses the expression of the AcrAB-TolC efflux pump, which is involved in the extrusion of a variety of antibiotics such as chloramphenicol (Ramos et al. 2005). Moreover, a sequence homologous to the *acrR* gene was found to be close to the *xenB* gene in *Pseudomonas fluorescens* I-C, which encodes a xenobiotic reductase B that degrades TNT in this bacterium (Blehert et al. 1999). Additionally, another gene found nearby the gene peg.1879 is one encoding an uncharacterized protein YhjG, which is homologous to a monooxygenase from *Bacillus subtilis* that participates in the initial step of the degradation of aromatic compounds (Nogales et al. 2017; MyBioSource 2023). It is also important to note that a transcriptional regulator of the LysR family was close to the gene peg.1879. Members belonging to this family are involved in several process such as the oxidative stress response and xenobiotic detoxification, including the regulation of genes encoding mexEF-OprN efflux pump, pirin, and dioxygenases that participate in aromatics degradation (Hihara et al. 2004; Díaz et al. 2013; Juarez 2017; Perez-Rueda et al. 2018; Henshke et al. 2021).

Furthermore, homologous sequences to hp_1879 were identified in UniProtKB, which revealed that this protein shares 76% identity with an intrinsically disordered protein (IDP) from *Pseudomonas* sp. BG5 (A0A7X6IP65). IDPs are functional proteins that lack a stable three-dimensional structure under physiological conditions and can adopt multiple conformational states (Trivedi and Nagarajaram 2022). IDPs often undergo induced folding upon binding to a specific partner such as proteins, nucleic acids, or small molecules (Uversky 2019).

The hypothetical protein hp_1879 is a low molecular mass protein with a theoretical mass of 17.5 kDa, which was calculated using the ExPASy's ProtParam tool (Gasteiger et al. 2005). In addition to this, it possesses characteristics typical of IDPs, such as a low proportion of hydrophobic and rigid residues, and high proportion of negatively charged and disorder-promoting residues (*e.g.*, Ala, Gly, Gln, and Ser). Given that IDPs have been implicated in membrane transport, such as porins (Novikova et al. 2021), and considering the aforementioned features, we propose that hp_1879 may be part of a transmembrane transporter involved in the extrusion of TNT and/or its metabolites.

Regarding the upregulated genes, peg.1078, peg.1079, and peg.1080, they encode hypothetical proteins (Table 1; Fig. S7) with amino acid sequences containing domains or motifs associated with membrane proteins according to UniProtKB. Notably, these proteins are remarkably small, comprising 59, 70, and 85 residues, respectively. Intriguingly, these genes are next to one encoding a 3-carboxymuconate cyclase, an enzyme involved in benzoate degradation through hydroxylation, and another encoding a 4-carboxymuconolactone decarboxylase, participating in the protocatechuate catabolism pathway, a route potentially involved in TNT degradation (Wells and Ragauskas 2012; Nogales et al. 2017; Xu et al. 2021). A transcription factor belonging to the LysR family was also found in the vicinity of the genes encoding these three hypothetical proteins. As mentioned above, members of this LyrR family are related to xenobiotic detoxification (Juarez 2017; Perez-Rueda et al. 2018; Henshke et al. 2021). The presence of such genes and their association with specific enzymes leads us to speculate that these hypothetical proteins might belong to the category of small membrane proteins. These are a relatively new subset of small (≤100 residues) bacterial proteins located in the cell membrane that can interact with and regulate other membrane proteins, such as drug efflux pumps, transporters, and receptors. Additionally, they play a regulatory role in various cellular processes, including stress response, signal transduction, respiration, and enzymatic activity (Yadavalli and Yuan 2022). Consequently, we believe that these hypothetical proteins in isolate TNT3 could be involved in the metabolism of TNT derivatives, potentially modulating the activity of enzymes participating in aromatic degradation pathways.

Downregulated DEGs in response to TNT exposure

Downregulation of multiple genes encoding pyrroloquinoline quinone (PQQ)-dependent enzymes associated with membranes, including alcohol and aldehyde dehydrogenases, and ABC transporters, was observed in TNT-treated samples (Table 3; Fig. S8). These proteins are involved in ethanol/aldehyde oxidation, a secondary pathway crucial for energy production and survival at low temperatures in certain bacteria, as evidenced in the Antarctic species *Pseudomonas extremaustralis* (Tribelli et al. 2015). It is plausible that the isolate TNT3 is unable to metabolize TNT and/or its metabolites via this pathway, leading to its downregulation. However, further research is required to elucidate the corresponding metabolic implications.

Moreover, several genes encoding the cytochrome *c* oxidase complex IV were significantly downregulated (Table 3; Fig. S8). Cytochrome *c* oxidase is a key enzyme in the electron

Table 3 List of the most downregulated DEGs in *Pseudomonas* sp. TNT3 grown in the presence of TNT

Process	Gene ID	RAST annotation	PROKKA annotation	Protein function	log_2FC
Alcohol oxidation	peg.974	Cytochrome c550, associated with quino(hemo) protein alcohol dehydrogenase (EC 1.1.99.8)	Quinohemoprotein alcohol dehydrogenase ADH IIB	Ethanol oxidation to acetaldehyde (Anthony and Williams 2003; Görisch 2003)	−6.3
	peg.980	Coenzyme PQQ synthesis protein B	Coenzyme PQQ synthesis protein B	Ethanol oxidation to acetaldehyde (Anthony and Williams 2003; Görisch 2003)	−5.1
	peg.975	Extracellular substrate-binding protein associated with quino(hemo)protein alcohol dehydrogenase	Membrane-bound lytic murein transglycosylase F	Ethanol oxidation to acetaldehyde (Anthony and Williams 2003; Görisch 2003)	−4.9
	peg.978	Quino(hemo)protein alcohol dehydrogenase, PQQ-dependent (EC 1.1.2.8)	Quinoprotein alcohol dehydrogenase (cytochrome c)	Ethanol oxidation to acetaldehyde (Anthony and Williams 2003; Görisch 2003)	−4.5
Electron transport chain	peg.3895	Cytochrome oxidase biogenesis protein Surf1, facilitates heme A insertion	Hypothetical protein	Heme *a* insertion (prosthetic group) into cytochrome *c* oxidase polypeptide I (Hannappel et al. 2012)	−4.5
	peg.3897	Cytochrome *c* oxidase polypeptide III (EC 1.9.3.1)	Cytochrome c oxidase subunit 3	Key role in energy production (Hederstedt 2022)	−4.4
	peg.3893	Heme A synthase, cytochrome oxidase biogenesis protein Cox15-CtaA	Heme A synthase	Heme A (prosthetic group of cytochrome *c* oxidase) synthesis from heme O group (Hederstedt 2022)	−4.0
	peg.3892	Heme O synthase, protoheme IX farnesyltransferase, COX10-CtaB	Protoheme IX farnesyltransferase	Conversion of heme B (protoheme IX) to heme O group, an intermediate to synthesize heme A (prosthetic group of cytochrome *c* oxidase) (Hederstedt 2022)	−3.8
	peg.3898	Cytochrome oxidase biogenesis protein Cox11-CtaG, copper delivery to Cox1	Cytochrome c oxidase assembly protein CtaG	Cytochrome *c* oxidase assembly factor (Hederstedt 2022)	−3.6
Motility	peg.5549	Flp pilus assembly protein TadC	Hypothetical protein	Flp (fimbrial low-molecular weight protein) pili-assembly (Alteri et al. 2022)	−3.7
	peg.5550	Flp pilus assembly protein TadB	Hypothetical protein	Flp (fimbrial low-molecular weight protein) pili-assembly (Alteri et al. 2022)	−3.5
	peg.5548	Flp pilus assembly protein TadD	Hypothetical protein	Secretion and export of the pilus (Li et al. 2019)	−3.0
	peg.5551	Type II/IV secretion system ATP hydrolase TadA/VirB11/CpaF, TadA subfamily	Putative conjugal transfer protein	Pilus secretion system (Planet et al. 2001)	−2.9
Unknown	peg.3894	Hypothetical protein	Hypothetical protein	Part of the cytochrome oxidase cluster?	−4.5
	peg.4610	Hypothetical protein	Hypothetical protein	Unknown	−4.3
	peg.3896	Hypothetical protein	Hypothetical protein	Small membrane protein that regulates methionine metabolism?	−4.0
	peg.5453	Hypothetical protein	Hypothetical protein	Unknown	−4.0

transport chain of bacteria, responsible for the final step in the aerobic respiration process (Hederstedt 2022). Previous studies have reported that exposure to xenobiotics can lead to the downregulation of cytochrome *c* oxidase expression in bacteria (Tribelli et al. 2015; Liu et al. 2017; Morales et al. 2021). The metabolic reprogramming that inhibits the electron transport chain to diminish ROS production during TNT exposure is a possible explanation for this downregulation.

Additionally, a set of genes encoding cell motility proteins and secretion systems, including the pilus assembly protein TadZ and the type II secretion system proteins, were significantly downregulated (Table 3; Fig. S8). Pilus-mediated motility machinery and translocation systems are closely interlaced, as the former entails the transportation of proteins across the cell envelope (Sato et al. 2010). The exposure to xenobiotics, in this case TNT, may incite changes in the bacterial cell membrane, thereby impacting intracellular signaling pathways of the regulatory cascade involved in the expression of genes related to motility. Moreover, xenobiotic exposure may activate stress response pathways in bacteria, prompting a redirection of cellular resources from non-essential processes (for survival) like pili formation to other critical cellular functions under these conditions. Thus, the expression of genes related to pili may be repressed to conserve energy and resources for more useful stress endurance routes. Consequently, the general motility of *Pseudomonas* sp. TNT3 may be affected when exposed to xenobiotics.

Concerning the downregulated DEGs encoding hypothetical proteins (Table 3), it was observed that the product of the gene peg.3894 shares 91% identity with a cytochrome *c* oxidase subunit from *Pseudomonas* sp. VI4.1 (UniProtKB: A0A1V4LGR9) and this gene is located within a cluster encoding proteins associated with the previously mentioned cytochrome *c* oxidase complex. Consequently, it is possible that this protein might have a structural role or be involved in the assembly of cytochrome *c* oxidase. Additionally, peg.3896 was found to encode a small protein comprising 67 residues, which shares 100% identity with a twin transmembrane helix small protein from *Pseudomonas* sp. TH10 (UniProtKB: A0A934T803). Notably, this hypothetical protein is situated adjacent to a methionine ABC transporter. These findings lead us to hypothesize that it could be a small membrane protein, as previously mentioned, potentially regulating the function of this transporter.

Conclusions

Here, we present for the first time a transcriptomic study of the response of an Antarctic bacterium, *Pseudomonas* sp. TNT3, to the exposure to the xenobiotic TNT. The investigation of the bacterium's gene expression profile following exposure to this compound revealed significant changes in a small set of genes. Our analysis demonstrates that compared to the control group, a significant proportion of differentially expressed genes were related to the metabolism of aromatics compounds, including phenylalanine, phenylacetate, and benzoate. These compounds are part of the "Xenobiotics biodegradation metabolism" pathway and were found to be overrepresented in both GO and KEGG enrichment analyses. Additionally, genes encoding efflux pumps and enzymes to cope with oxidative and thiol stress were also upregulated, which reinforces the bacterium's ability to adapt to the xenobiotic stress.

Notably, we identified an FMN-dependent NADH-azoreductase gene that was the most upregulated among all genes analyzed. This type of enzyme is known to be capable of degrading TNT and has been reported in a few transcriptomic studies but has not yet been classified into any xenobiotic degradation pathway.

The present study's results further highlight the complexity of the metabolic machinery involved in the xenobiotic stress response, which is poorly understood due to the rapid reassignment of transcriptional elements from dispensable functions required for tolerance to environmental stressors. Our study's findings add to the growing body of knowledge on bacterial responses to xenobiotic stress and pave the way for further research on the mechanisms involved in xenobiotic degradation pathways.

Supplementary Information The online version contains supplementary material available at https://doi.org/10.1007/s11356-024-32298-x.

Acknowledgements All authors acknowledge Dr. Carolina P. Quezada for facilitating the soil samples from Deception Island and the Chilean Army for their constant support and help, particularly Mr. Martín Inzunza and CIMI (Comando de Industria Militar e Ingeniería del Ejército de Chile). The authors also acknowledge Erika Elcira Donoso López.

Author contribution The study was designed and conceived by Ma. Ángeles Cabrera, Sebastián L. Márquez, and José M. Pérez-Donoso. The experimental work was performed by Ma. Ángeles Cabrera. Data processing and curation were performed by Sebastián L. Márquez. Data analysis was performed by Ma. Ángeles Cabrera and Sebastián L. Márquez. The first draft of the manuscript was prepared by Ma. Ángeles Cabrera and Sebastián L. Márquez. José M. Pérez-Donoso acquired the funding, revised, and critically discussed the manuscript. All authors have commented on earlier versions of the manuscript. All authors read and approved the final manuscript.

Funding This work was supported by the US Army Research, Development and Engineering Command (RDECOM US Army, W911NF-17–2-0156), Fondo Nacional de Desarrollo Científico y Tecnológico (FONDECYT 1200870), and Instituto Antártico Chileno, Expedición Chilena Antártica No. 54 (INACH, RT_25-16).

Data availability The raw transcriptome data were deposited in the Sequence Read Archive (SRA) database of National Center for Biotechnology Information (NCBI) under the accession number PRJNA975916 (BioProject).

Declarations

Ethics approval Not applicable.

Consent to participate All authors consent to participate in the manuscript.

Consent for publication All authors consent to submit and publish the manuscript.

Competing interests The authors declare no competing interests.

References

Adams M, Jia Z (2005) Structural and biochemical analysis reveal pirins to possess quercetinase activity. J Biol Chem 280:28675–28682. https://doi.org/10.1074/JBC.M501034200

Aldarini N, Alhasawi AA, Thomas SC, Appanna VD (2017) The role of glutamine synthetase in energy production and glutamine metabolism during oxidative stress. Antonie Van Leeuwenhoek 110:629–639. https://doi.org/10.1007/S10482-017-0829-3/METRICS

Allocati N, Federici L, Masulli M, Di Ilio C (2009) Glutathione transferases in bacteria. FEBS J 276:58–75. https://doi.org/10.1111/J.1742-4658.2008.06743.X

Alteri CJ, Rios-Sarabia N, De la Cruz MA et al (2022) The Flp type IV pilus operon of *Mycobacterium tuberculosis* is expressed upon interaction with macrophages and alveolar epithelial cells. Front Cell Infect Microbiol 12:916247. https://doi.org/10.3389/FCIMB.2022.916247/FULL

Anders S, Pyl PT, Huber W (2015) HTSeq-A Python framework to work with high-throughput sequencing data. Bioinformatics 31:166–169. https://doi.org/10.1093/bioinformatics/btu638

Anthony C, Williams P (2003) The structure and mechanism of methanol dehydrogenase. Biochim Biophys Acta - Proteins Proteomics 1647:18–23. https://doi.org/10.1016/S1570-9639(03)00042-6

ATSDR (2022) ATSDR's substance priority list. In: Agency Toxic Subst. Dis. Regist. https://www.atsdr.cdc.gov/spl/index.html#2022spl. Accessed 8 Nov 2023

Bateman A, Martin MJ, Orchard S et al (2023) UniProt: the universal protein knowledgebase in 2023. Nucleic Acids Res 51:D523–D531. https://doi.org/10.1093/NAR/GKAC1052

Blehert DS, Fox BG, Chambliss GH (1999) Cloning and sequence analysis of two *Pseudomonas* flavoprotein xenobiotic reductases. J Bacteriol 181:6254–6263

Brown NL, Stoyanov JV, Kidd SP, Hobman JL (2003) The MerR family of transcriptional regulators. FEMS Microbiol Rev 27:145–163. https://doi.org/10.1016/S0168-6445(03)00051-2

Bushnell B (2015) BBMap (version 37.75) [Software]. Available at https://sourceforge.net/projects/bbmap/

Cabrera MÁ, Márquez SL, Quezada CP et al (2020) Biotransformation of 2,4,6-trinitrotoluene by *Pseudomonas* sp. TNT3 isolated from Deception Island, Antarctica. Environ Pollut 262:113922. https://doi.org/10.1016/j.envpol.2020.113922

Cabrera MÁ, Márquez SL, Pérez-Donoso JM (2022) Comparative genomic analysis of Antarctic *Pseudomonas* isolates with 2,4,6-trinitrotoluene transformation capabilities reveals their unique features for xenobiotics degradation. Genes (basel) 13:1354. https://doi.org/10.3390/GENES13081354/S1

Carbon S, Douglass E, Good BM et al (2021) The Gene Ontology resource: enriching a GOld mine. Nucleic Acids Res 49:D325–D334. https://doi.org/10.1093/nar/gkaa1113

Chakraborty N, Begum P, Patel BK (2022) Counterbalancing common explosive pollutants (TNT, RDX, and HMX) in the environment by microbial degradation. In: Rodriguez-Couto S, Shah MP (eds) Development in Wastewater Treatment Research and Processes. Elsevier, pp 263–310. https://doi.org/10.1016/B978-0-323-85839-7.00012-8. Accessed 22 Mar 2023

Chen L, Xie QW, Nathan C (1998) Alkyl hydroperoxide reductase subunit C (AhpC) protects bacterial and human cells against reactive nitrogen intermediates. Mol Cell 1:795–805. https://doi.org/10.1016/S1097-2765(00)80079-9

Cho YS, Lee BU, Kahng HY, Oh KH (2009) Comparative analysis of 2,4,6-trinitrotoluene (TNT)-induced cellular responses and proteomes in *Pseudomonas* sp. HK-6 in two types of media. J Microbiol 47:220–224. https://doi.org/10.1007/s12275-008-0108-0

Claus H (2014) Microbial degradation of 2,4,6-trinitrotoluene *in vitro* and in natural environments. In: Singh SN (ed) Biological remediation of explosive residues. Springer International Publishing, Cham, pp 15–38

Danecek P, Bonfield JK, Liddle J et al (2021) Twelve years of SAMtools and BCFtools. Gigascience 10. https://doi.org/10.1093/gigascience/giab008

De Jong A, Kuipers OP, Kok J (2022) FUNAGE-Pro: comprehensive web server for gene set enrichment analysis of prokaryotes. Nucleic Acids Res 50:W330–W336. https://doi.org/10.1093/NAR/GKAC441

Díaz E, Jiménez JI, Nogales J (2013) Aerobic degradation of aromatic compounds. Curr Opin Biotechnol 24:431–442. https://doi.org/10.1016/j.copbio.2012.10.010

Durante-Rodríguez G, Gómez-Álvarez H, Nogales J et al (2017) One-component systems that regulate the expression of degradation pathways for aromatic compounds. In: Krell T (ed) Cellular ecophysiology of microbe. Springer International Publishing, Cham, pp 1–39

Esteve-Núñez A, Caballero A, Ramos JL (2001) Biological degradation of 2,4,6-trinitrotoluene. Microbiol Mol Biol Rev 65:335–352. https://doi.org/10.1128/MMBR.65.3.335

Fernández M, Duque E, Pizarro-Tobías P et al (2009) Microbial responses to xenobiotic compounds. Identification of genes that allow *Pseudomonas putida* KT2440 to cope with 2,4,6-trinitrotoluene. Microb Biotechnol 2:287–294. https://doi.org/10.1111/j.1751-7915.2009.00085.x

Fetar H, Gilmour C, Klinoski R et al (2011) mexEF-oprN multidrug efflux operon of *Pseudomonas aeruginosa*: regulation by the MexT activator in response to nitrosative stress and chloramphenicol. Antimicrob Agents Chemother 55:508–514. https://doi.org/10.1128/AAC.00830-10

Galperin MY, Wolf YI, Makarova KS et al (2021) COG database update: focus on microbial diversity, model organisms, and widespread pathogens. Nucleic Acids Res 49:D274–D281. https://doi.org/10.1093/nar/gkaa1018

Ganesh Kumar A, Mathew NC, Sujitha K et al (2019) Genome analysis of deep sea piezotolerant *Nesiotobacter exalbescens* COD22 and toluene degradation studies under high pressure condition. Sci Rep 9:18724. https://doi.org/10.1038/s41598-019-55115-9

Gasteiger E, Hoogland C, Gattiker A et al (2005) Protein identification and analysis tools on the ExPASy server. In: Walker JM (ed) The proteomics protocols handbook. Humana Press, Totowa, pp 571–607

Gonçalves AMD, Mendes S, De Sanctis D et al (2013) The crystal structure of *Pseudomonas putida* azoreductase — the active site revisited. FEBS J 280:6643–6657. https://doi.org/10.1111/FEBS.12568/FORMAT/PDF

Görisch H (2003) The ethanol oxidation system and its regulation in *Pseudomonas aeruginosa*. Biochim Biophys Acta 1647:98–102. https://doi.org/10.1016/S1570-9639(03)00066-9

Grishin AM, Cygler M (2015) Structural Organization of Enzymes of the Phenylacetate Catabolic Hybrid Pathway. Biology (Basel) 4:424–442. https://doi.org/10.3390/BIOLOGY4020424

Gupta S, Goel SS, Ramanathan G, Ronen Z (2023a) Biotransformation of 2,4,6-trinitrotoluene by *Diaphorobacter* sp. strain DS2. Environ Sci Pollut Res 30:120749–120762. https://doi.org/10.1007/s11356-023-30651-0

Gupta S, Goel SS, Siebner H et al (2023b) Transformation of 2, 4, 6-trinitrotoluene by *Stenotrophomonas* strain SG1 under aerobic and anaerobic conditions. Chemosphere 311:137085. https://doi.org/10.1016/j.chemosphere.2022.137085

Habineza A, Zhai J, Mai T et al (2017) Biodegradation of 2, 4, 6-trinitrotoluene (TNT) in contaminated soil and microbial remediation options for treatment. Period Polytech Chem Eng 61:171–187. https://doi.org/10.3311/PPch.9251

Haïdour A, Ramos JL (1996) Identification of products resulting from the biological reduction of 2,4,6-trinitrotoluene, 2,4-dinitrotoluene, and 2,6-dinitrotoluene by *Pseudomonas* sp. Environ Sci Technol 30:2365–2370. https://doi.org/10.1021/es950824u

Hannappel A, Bundschuh FA, Ludwig B (2012) Role of Surf1 in heme recruitment for bacterial COX biogenesis. Biochim Biophys Acta - Bioenerg 1817:928–937. https://doi.org/10.1016/J.BBABIO.2011.09.007

Hawari J, Beaudet S, Halasz A et al (2000) Microbial degradation of explosives: biotransformation versus mineralization. Appl Microbiol Biotechnol 54:605–618. https://doi.org/10.1007/s002530000445

Hederstedt L (2022) Diversity of cytochrome c oxidase assembly proteins in bacteria. Microorganisms 10:926. https://doi.org/10.3390/MICROORGANISMS10050926

Heiss G, Knackmuss H-J (2002) Bioelimination of trinitroaromatic compounds: immobilization versus mineralization. Curr Opin Microbiol 5:282–287

Henshke Y, Shemer B, Belkin S (2021) The *Escherichia coli* azoR gene promoter: a new sensing element for microbial biodetection of trace explosives. Curr Res Biotechnol 3:21–28. https://doi.org/10.1016/j.crbiot.2021.01.003

Hihara Y, Muramatsu M, Nakamura K, Sonoike K (2004) A cyanobacterial gene encoding an ortholog of Pirin is induced under stress conditions. FEBS Lett 574:1–3. https://doi.org/10.1016/j.febslet.2004.06.102

Ho EM, Chang HW, Il KS et al (2004) Analysis of TNT (2,4,6-trinitrotoluene)-inducible cellular responses and stress shock proteome in *Stenotrophomonas* sp. OK-5. Curr Microbiol 49:346–352. https://doi.org/10.1007/s00284-004-4322-7

Johnson GR, Smets BF, Spain JC (2001) Oxidative transformation of aminodinitrotoluene isomers by multicomponent dioxygenases. Appl Environ Microbiol 67:5460–5466. https://doi.org/10.1128/AEM.67.12.5460-5466.2001

Juarez P (2017) Regulatory mechanisms of mexEF-oprN efflux operon in *Pseudomonas aeruginosa*: from mutations in clinical isolates to its induction as response to electrophilic stress. Université Bourgogne Franche-Comté. https://theses.hal.science/tel-01842272v1/document

Kanehisa M, Furumichi M, Sato Y et al (2023) KEGG for taxonomy-based analysis of pathways and genomes. Nucleic Acids Res 51:D587–D592. https://doi.org/10.1093/NAR/GKAC963

Kao CM, Lin BH, Chen SC et al (2016) Biodegradation of trinitrotoluene (TNT) by indigenous microorganisms from TNT-contaminated soil, and their application in TNT bioremediation. Bioremediat J 20:165–173. https://doi.org/10.1080/10889868.2016.1148007

Keenan BG, Wood TK (2006) Orthric Rieske dioxygenases for degrading mixtures of 2,4-dinitrotoluene/ naphthalene and 2-amino-4,6-dinitrotoluene/4-amino-2,6-dinitrotoluene. Appl Microbiol Biotechnol 73:827–838. https://doi.org/10.1007/s00253-006-0538-8

Kim HY, Bennett GN, Song HG (2002) Degradation of 2,4,6-trinitrotoluene by *Klebsiella* sp. isolated from activated sludge. Biotechnol Lett 24:2023–2028. https://doi.org/10.1023/A:1021127201608

Koske D, Goldenstein NI, Kammann U (2019) Nitroaromatic compounds damage the DNA of zebrafish embryos (*Danio rerio*). Aquat Toxicol 217:105345. https://doi.org/10.1016/j.aquatox.2019.105345

Kumagai Y, Shimojo N (2002) Possible mechanisms for induction of oxidative stress and suppression of systemic nitric oxide production caused by exposure to environmental chemicals. Environ Health Prev Med 7:141–150. https://doi.org/10.1265/ehpm.2002.141

Ladino-Orjuela G, Gomes E, da Silva R et al (2016) Metabolic pathways for degradation of aromatic hydrocarbons by bacteria. Rev Environ Contam Toxicol 237:105–121. https://doi.org/10.1007/978-3-319-23573-8_5

Lamba J, Anand S, Dutta J, Rai PK (2022) 2,4,6-trinitrotoluene (TNT) degradation by *Indiicoccus explosivorum* (S5-TSA-19). Arch Microbiol 204:447. https://doi.org/10.1007/s00203-022-03057-8

Langmead B, Salzberg SL (2012) Fast gapped-read alignment with Bowtie 2. Nat Methods 9:357–359. https://doi.org/10.1038/nmeth.1923

Lata K, Kushwaha A, Ramanathan G (2021) Chapter 23 — Bacterial enzymatic degradation and remediation of 2,4,6-trinitrotoluene. In: Das S, Dash HR (eds) Microbial and natural macromolecules. Academic Press, pp 623–659. https://doi.org/10.1016/B978-0-12-820084-1.00024-7

Li T, Zhang Q, Wang R et al (2019) The roles of flp1 and tadD in *Actinobacillus pleuropneumoniae* pilus biosynthesis and pathogenicity. Microb Pathog 126:310–317. https://doi.org/10.1016/J.MICPATH.2018.11.010

Liao HY, Chien CC, Tang P et al (2018) The integrated analysis of transcriptome and proteome for exploring the biodegradation mechanism of 2, 4, 6-trinitrotoluene by *Citrobacter* sp. J Hazard Mater 349:79–90. https://doi.org/10.1016/j.jhazmat.2018.01.039

Liu G, Zhou J, Lv H et al (2007) Azoreductase from *Rhodobacter sphaeroides* AS1.1737 is a flavodoxin that also functions as nitroreductase and flavin mononucleotide reductase. Appl Microbiol Biotechnol 76:1271–1279. https://doi.org/10.1007/s00253-007-1087-5

Liu X, Shen B, Du P et al (2017) Transcriptomic analysis of the response of *Pseudomonas fluorescens* to epigallocatechin gallate by RNA-seq. PLoS One 12:e0177938. https://doi.org/10.1371/JOURNAL.PONE.0177938

Love MI, Huber W, Anders S (2014) Moderated estimation of fold change and dispersion for RNA-seq data with DESeq2. Genome Biol 15:550. https://doi.org/10.1186/s13059-014-0550-8

Luengo JM, García JL, Olivera ER (2001) The phenylacetyl-CoA catabolon: a complex catabolic unit with broad biotechnological applications. Mol Microbiol 39:1434–1442. https://doi.org/10.1046/j.1365-2958.2001.02344.x

Maksimova YG, Maksimov AY, Demakov VA (2018) Biotechnological approaches to the bioremediation of an environment polluted with trinitrotoluene. Appl Biochem Microbiol 54:767–779. https://doi.org/10.1134/S0003683818080045

Mercier C, Chalansonnet V, Orenga S, Gilbert C (2013) Characteristics of major *Escherichia coli* reductases involved in aerobic nitro and

azo reduction. J Appl Microbiol 115:1012–1022. https://doi.org/10.1111/jam.12294
Mercimek HA, Dincer S, Guzeldag G et al (2013) Aerobic biodegradation of 2,4,6-trinitrotoluene (TNT) by *Bacillus cereus* isolated from contaminated soil. Microb Ecol 66:512–521. https://doi.org/10.1007/s00248-013-0248-6
Misal SA, Gawai KR (2018) Azoreductase: a key player of xenobiotic metabolism. Bioresour Bioprocess 5:17
Morales M, Sentchilo V, Hadadi N, van der Meer JR (2021) Genome-wide gene expression changes of *Pseudomonas veronii* 1YdBTEX2 during bioaugmentation in polluted soils. Environ Microbiome 16:8. https://doi.org/10.1186/s40793-021-00378-x
Mordor-Intelligence (2021) Trinitrotoluene (TNT) market - Growth, trends, COVID-19 impact, and forecasts (2022 - 2027). https://www.mordorintelligence.com/industry-reports/trinitrotoluene-market
Moussatova A, Kandt C, O'Mara ML, Tieleman DP (2008) ATP-binding cassette transporters in *Escherichia coli*. Biochim Biophys Acta - Biomembr 1778:1757–1771. https://doi.org/10.1016/J.BBAMEM.2008.06.009
MyBioSource (2023) yhjG recombinant protein: uncharacterized aromatic compound monooxygenase yhjG. https://www.mybiosource.com/recombinant-protein/uncharacterized-aromatic-compound-monooxygenase-yhjg-yhjg/1115304
Nogales J, García JL, Díaz E (2017) Degradation of aromatic compounds in *Pseudomonas*: a systems biology view. In: Rojo F (ed) Aerobic utilization of hydrocarbons, oils, and lipids. Handbook of hydrocarbon and lipid microbiology. Springer International Publishing, Cham, pp 1–49
Novikova OD, Uversky VN, Zelepuga EA (2021) Non-specific porins of Gram-negative bacteria as proteins containing intrinsically disordered regions with amyloidogenic potential. Prog Mol Biol Transl Sci 183:75–99. https://doi.org/10.1016/BS.PMBTS.2021.06.012
Ortiz-Hernández ML, Gama-Martínez Y, Fernández-López M et al (2021) Transcriptomic analysis of Burkholderia cenocepacia CEIB S5–2 during methyl parathion degradation. Environ Sci Pollut Res 28:42414–42431. https://doi.org/10.1007/s11356-021-13647-6
Paysan-Lafosse T, Blum M, Chuguransky S et al (2023) InterPro in 2022. Nucleic Acids Res 51:D418–D427. https://doi.org/10.1093/NAR/GKAC993
Perez-Rueda E, Hernandez-Guerrero R, Alberto Martinez-Nuñez M et al (2018) Abundance, diversity and domain architecture variability in prokaryotic DNA-binding transcription factors. PLoS One 13:e0195332. https://doi.org/10.1371/journal.pone.0195332
Planet PJ, Kachlany SC, DeSalle R, Figurski DH (2001) Phylogeny of genes for secretion NTPases: Identification of the widespread tadA subfamily and development of a diagnostic key for gene classification. Proc Natl Acad Sci 98:2503–2508. https://doi.org/10.1073/pnas.051436598
Poole K (2012) Bacterial stress responses as determinants of antimicrobial resistance. J Antimicrob Chemother 67:2069–2089. https://doi.org/10.1093/jac/dks196
Ramos JL, Martínez-Bueno M, Molina-Henares AJ et al (2005) The TetR family of transcriptional repressors. Microbiol Mol Biol Rev 69:326–356. https://doi.org/10.1128/MMBR.69.2.326-356.2005
Rocha ER, Smith CJ (1999) Role of the alkyl hydroperoxide reductase (ahpCF) gene in oxidative stress defense of the obligate anaerobe *Bacteroides fragilis*. J Bacteriol 181:5701–5710
Sato K, Naito M, Yukitake H et al (2010) A protein secretion system linked to bacteroidete gliding motility and pathogenesis. Proc Natl Acad Sci 107:276–281. https://doi.org/10.1073/pnas.0912010107
Schneider BL, Hernandez VJ, Reitzer L (2013) Putrescine catabolism is a metabolic response to several stresses in *Escherichia coli*. Mol Microbiol 88:537–550. https://doi.org/10.1016/j.biotechadv.2011.08.021.Secreted
Seaver LC, Imlay JA (2001) Alkyl hydroperoxide reductase is the primary scavenger of endogenous hydrogen peroxide in *Escherichia coli*. J Bacteriol 183:7173–7181. https://doi.org/10.1128/JB.183.24.7173-7181.2001/ASSET/CB26C1A6-FA27-4E38-A8AD-D1BB31671DB1/ASSETS/GRAPHIC/JB2410846005.JPEG
Shen CF, Hawari JA, Ampleman G et al (2000) Origin of p-cresol in the anaerobic degradation of trinitrotoluene. Can J Microbiol 46:119–124. https://doi.org/10.1139/cjm-46-2-119
Solmi L, Rossi FR, Romero FM et al (2023) Polyamine-mediated mechanisms contribute to oxidative stress tolerance in *Pseudomonas syringae*. Sci Rep 13:4279. https://doi.org/10.1038/s41598-023-31239-x
Talà A, Damiano F, Gallo G et al (2018) Pirin: a novel redox-sensitive modulator of primary and secondary metabolism in *Streptomyces*. Metab Eng 48:254–268. https://doi.org/10.1016/j.ymben.2018.06.008
Tan J, Kan N, Wang W et al (2015) Construction of 2,4,6-trinitrotoluene biosensors with novel sensing elements from *Escherichia coli* K-12 MG1655. Cell Biochem Biophys 72:417–428. https://doi.org/10.1007/s12013-014-0481-8
Teufel R, Mascaraque V, Ismail W et al (2010) Bacterial phenylalanine and phenylacetate catabolic pathway revealed. Proc Natl Acad Sci 107:14390–14395. https://doi.org/10.1073/pnas.1005399107
Thenmozhi A, Devasena M (2020) Remediation of 2,4,6-trinitrotoluene persistent in the environment — a review. Soil Sediment Contam an Int J 29:1–13. https://doi.org/10.1080/15320383.2019.1664394
Thomas C, Tampé R (2020) Structural and mechanistic principles of ABC transporters. Annu Rev Biochem 89:605–636. https://doi.org/10.1146/annurev-biochem-011520-105201
Tribelli PM, Venero ECS, Ricardi MM et al (2015) Novel essential role of ethanol oxidation genes at low temperature revealed by transcriptome analysis in the Antarctic bacterium *Pseudomonas extremaustralis*. PLoS One 10:e0145353. https://doi.org/10.1371/journal.pone.0145353
Trivedi R, Nagarajaram HA (2022) Intrinsically disordered proteins — an overview. Int J Mol Sci 23:14050. https://doi.org/10.3390/IJMS232214050
Uversky VN (2019) Intrinsically disordered proteins and their "mysterious" (meta)physics. Front Phys 7:10. https://doi.org/10.3389/fphy.2019.00010
Van Dillewijn P, Caballero A, Paz J et al (2007) Bioremediation of 2,4,6-trinitrotoluene under field conditions. Environ Sci Technol 41:1378–1383. https://doi.org/10.1021/ES062165Z
Wang Y (2022) Pirin, a multifunction protein with quercetinase activity and involvement in transcription regulation. Int J Biosci Biochem Bioinforma 12:85–92. https://doi.org/10.17706/IJBBB.2022.12.4.85-92
Wells T, Ragauskas AJ (2012) Biotechnological opportunities with the β-ketoadipate pathway. Trends Biotechnol 30:627–637. https://doi.org/10.1016/j.tibtech.2012.09.008
Widiatningrum T, Maeda S, Kataoka K, Sakurai T (2015) A pirin-like protein from *Pseudomonas stutzeri* and its quercetinase activity. Biochem Biophys Rep 3:144–149. https://doi.org/10.1016/J.BBREP.2015.08.001
Xiong A, Gottman A, Park C et al (2000) The EmrR protein represses the *Escherichia coli emrRAB* multidrug resistance operon by directly binding to its promoter region. Antimicrob Agents Chemother 44:2905. https://doi.org/10.1128/AAC.44.10.2905-2907.2000
Xu M, Liu D, Sun P et al (2021) Degradation of 2,4,6-trinitrotoluene (TNT): involvement of protocatechuate 3,4-dioxygenase (P34O) in Buttiauxella sp. S19–1. Toxics 9:231. https://doi.org/10.3390/toxics9100231

Xu M, He L, Sun P et al (2023) Critical role of monooxygenase in biodegradation of 2,4,6-trinitrotoluene by Buttiauxella sp. S19–1. Molecules 28:1969. https://doi.org/10.3390/molecules28041969
Yadavalli SS, Yuan J (2022) Bacterial small membrane proteins: the Swiss army knife of regulators at the lipid bilayer. J Bacteriol 204:e00344-e421. https://doi.org/10.1128/JB.00344-21
Yakovleva G, Kurdy W, Gorbunova A et al (2022) *Bacillus pumilus* proteome changes in response to 2,4,6-trinitrotoluene-induced stress. Biodegradation 33:593–607. https://doi.org/10.1007/s10532-022-09997-8
Yu G, Wang LG, Han Y, He QY (2012) ClusterProfiler: An R package for comparing biological themes among gene clusters. Omi A J Integr Biol 16:284–287. https://doi.org/10.1089/omi.2011.0118
Zgurskaya HI (2009) Multicomponent drug efflux complexes: architecture and mechanism of assembly. Future Microbiol 4:919. https://doi.org/10.2217/FMB.09.62